Singular BEM and its Application to 3D Electrical Impedance Tomography

N.A. Gumerov and G.L. Chahine
DYNAFLOW, INC., *7210 Pindell School Road, Fulton, MD 20759*
E-mail: info@dynaflow-inc.com, http://www.dynaflow-inc.com

1 Introduction

In Electrical Impedance Tomography (EIT) the distribution of conductivity inside a container is sought by applying specified currents (or voltages) at some parts of the container surface, and performing measurements of the voltage (or current) of some other parts. The equations for the electric field then provide relationships between the conductivity distribution inside the domain and the measured voltages and currents. Different types of materials have different conductivity, and the availability of a conductivity map provides an image of the material distribution in the container.

An efficient reconstruction algorithm based on the Boundary Element Method (BEM) was proposed recently [1]. Minimization procedures used for EIT usually require a large number of calls to the forward problem solver whose efficiency determines the efficiency of the problem solution. The objective of the present study is to optimize the forward problem solver. We limit ourselves to the problem of detection of regions of zero conductivity (such as cavities or cracks) inside an imaged 3D object. In this case the forward problem is a Neumann problem for the Laplace equation. To avoid the need for computational mesh refinement near the electrodes we model these as point singularities on the object surface. If these singularities are not treated properly considerable errors are introduced in the BEM solution. Here we propose a solution method, the 'singular BEM', which showed good performance.

2 Forward EIT Problem

Consider a 3D region Ω occupied by material of constant conductivity σ with one or several embedded objects of zero conductivity. We use N electrodes with centers $\mathbf{x}_1, ..., \mathbf{x}_N$ located on the boundary of Ω to inject current and measure voltages and one reference electrode $\mathbf{x}_{N+1}$. All potential measurements are made with respect to the reference electrode. In a number of problems the size of the electrodes is very small compared with the size of the domain. In this case we introduce the concept of a point electrode. This concept enables substantial savings in computation time. The point electrode approximation treats the electrodes as singularities (sinks and sources) at the boundary of the domain. In this case the electrical potential distribution, ϕ^{ij},

generated by the current, I, injected through a pair of electrodes i and j can be determined by solving the following problem

$$\sigma \nabla^2 \phi^{ij} = 2\pi I \left[\delta \left(\mathbf{x} - \mathbf{x}_i \right) - \delta \left(\mathbf{x} - \mathbf{x}_j \right) \right], \tag{1}$$

$$\left. \frac{\partial \phi^{ij}}{\partial n} \right|_S = 0, \qquad \left. \phi^{ij} \right|_{\mathbf{x}=\mathbf{x}_{N+1}} = 0, \qquad i, j = 1, ..., N, \tag{2}$$

where S is the entire surface of the domain of conductivity σ consisting of the surface of the embedded objects and the external boundary of Ω excluding points $\mathbf{x}_i$. δ is the Dirac delta function. The forward EIT problem is to solve equations (1)-(2).

3 Decomposition of the Solution

Now, consider the following problem

$$\nabla^2 \Phi_i = 2\pi \left[\delta \left(\mathbf{x} - \mathbf{x}_i \right) - \delta \left(\mathbf{x} - \mathbf{x}_{int} \right) \right], \tag{3}$$

$$\left. \frac{\partial \Phi_i}{\partial n} \right|_S = 0, \qquad \left. \Phi_i \right|_{\mathbf{x}=\mathbf{x}_{N+1}} = 0, \qquad i = 1, ..., N, \tag{4}$$

where $\mathbf{x}_{int}$ is an arbitrary point *inside* the domain. Because the problem (1)-(2) is linear, we can decompose ϕ^{ij} as:

$$\phi^{ij} = \frac{I}{\sigma} \left(\Phi_i - \Phi_j \right), \qquad i, j = 1, ..., N. \tag{5}$$

This simple step is important since it reduces by a factor of N the number of equations to solve and allows to implement the singular BEM.

4 BEM for Point Electrodes

The problem (3)-(4) can be reformulated via *Green's identity:*

$$a\pi \Phi_i(\mathbf{x}) = a\pi \left[G \left(\mathbf{x}, \mathbf{x}_{int} \right) - G(\mathbf{x}, \mathbf{x}_i) \right] + \int_S \Phi_i(\mathbf{y}) \frac{\partial G}{\partial n}(\mathbf{x}, \mathbf{y}) dS. \tag{6}$$

where a is the solid angle under which the point $\mathbf{x}$ sees the rest of the domain, and G is Green's function,

$$G(\mathbf{x}, \mathbf{y}) = - \left| \mathbf{x} - \mathbf{y} \right|^{-1}. \tag{7}$$

The surface integrals can then be performed by suitably discretizing the boundaries. Here we use plane triangular elements $\{S_m\}$, $m = 1, ..., M$. Over each sub-domain S_m a linear Lagrangian interpolation of Φ_i is performed using the values at the nodes (triangle vertices). The resultant boundary integrals can then be calculated, leading to a discrete relation between the values of Φ_i at points $\mathbf{x}$, and the values of Φ_i on the element nodes. Following a collocation approach, by selecting the points $\mathbf{x}$ to be the nodes on S, we obtain the following linear system of equations:

$$\mathbf{B} \Phi_i = a\pi \left[G \left(\mathbf{x}_l, \mathbf{x}_i \right) - G(\mathbf{x}_l, \mathbf{x}_{int}) \right], \qquad i = 1, ..., N, \qquad l = 1, ..., L \tag{8}$$

$\mathbf{B}$ is a matrix corresponding to the integrations with the derivative of Green's function [1]. Note that the concept of point electrodes avoids integration the normal derivative of Φ_i (since it is zero) and saves CPU time.

5 Singular BEM

In the absence of current injection, equation (8) becomes $\mathbf{B\Phi} = \mathbf{0}$, which has as solution $\Phi = const$. In discrete form $\Phi = const$ corresponds to the following vector $\mathbf{\Phi}$:

$$\mathbf{\Phi} = const \cdot \mathbf{U}, \qquad \mathbf{U} = \begin{pmatrix} 1 \\ 1 \\ \dots \\ 1 \end{pmatrix}. \tag{9}$$

and

$$\mathbf{B\Phi} = \mathbf{0} \Longrightarrow \mathbf{BU} = \mathbf{0}, \tag{10}$$

Normally, due to the errors of discretization the computed elements of $\mathbf{B}$ do not satisfy exactly (10). So we force the diagonal elements to be

$$B_{kk} = -(B_{k1} + ... + B_{k-1,1} + B_{k+1,1} + ... + B_{kL}), \qquad k = 1, ..., L, \tag{11}$$

where L is the number of collocation points and satisfy (10).

Consider now the non-uniform equation:

$$\mathbf{B\Phi}_i = \mathbf{Y}, \tag{12}$$

with an arbitrary right hand side vector $\mathbf{Y}$. Due to Condition (10) this equation has a solution if and only if the vector $\mathbf{Y}$ is orthogonal to the vector $\mathbf{U}$, or

$$(\mathbf{Y} \cdot \mathbf{U}) = Y_1 + Y_2 + ... + Y_L = 0. \tag{13}$$

Now let us select the collocation points in such a way that the point electrodes including the reference electrode belong to the collocation point set. In this case the right hand side of (8) is singular only for $\mathbf{x}_l = \mathbf{x}_i$. Let us define now the vector $\mathbf{Y}$ as follows:

$$\begin{aligned} Y_l &= a\pi \left[G\left(\mathbf{x}_l, \mathbf{x}_i\right) - G(\mathbf{x}_l, \mathbf{x}_{int})\right], \quad \text{if } \mathbf{x}_l \neq \mathbf{x}_i, \\ Y_l &= -\left(Y_1 + ... + Y_{l-1} + Y_{l+1} + ... + Y_L\right), \quad \text{if } \mathbf{x}_l = \mathbf{x}_i. \end{aligned} \tag{14}$$

This determines a non-singular vector $\mathbf{Y}$ satisfying the orthogonality condition (13) required for existence of the solution. To make the solution unique we impose the zero condition at the point $\mathbf{x}_{N+1}$ (4) and modify the matrix $\mathbf{B}$ and the vector $\mathbf{Y}$ as follows:

$$B_{lm}^{(\mathrm{mod})} = \begin{cases} B_{lm}, & \text{if } l \neq N+1 \text{ and } m \neq N+1 \\ 0, & \text{if } l = N+1 \text{ or } m = N+1 \\ 1, & \text{if } l = N+1 \text{ and } m = N+1 \end{cases}, \quad Y_l^{(\mathrm{mod})} = \begin{cases} Y_l, & \text{if } l \neq N+1 \\ 0, & \text{if } l = N+1 \end{cases}. \tag{15}$$

The modified matrix $\mathbf{B}^{(\mathrm{mod})}$ now has a non-zero determinant and the unique solution of equation

$$\mathbf{B}^{(\mathrm{mod})}\mathbf{\Phi}_i = \mathbf{Y}^{(\mathrm{mod})}. \tag{16}$$

provides a numerical solution of the problem (3)-(4).

The essence of the singular BEM is a modification of the right hand side vector (14) by placing the source at a collocation point and the imposition of the condition of orthogonality, which leads to a unique solution of the equations.

6 Inverse EIT Problem

The inverse EIT problem is to determine the shapes and locations of the embedded objects using data on measured potentials at all combinations of the injection electrodes. To solve this problem we parametrize the position and shape of each embedded object with several parameters. The total number of parameters (dimension of the vector of parameters, $\mathbf{p}$) depends on the number of objects and on the required accuracy in the shape determination. For example, if an embedded object can be approximated with a sphere it requires 4 parameters (three coordinates of the sphere center, and the radius); the approximation of the shape with an ellipsoid requires 9 parameters, etc. To find the $\mathbf{p}$ which fits best the measured data, we use a multidimensional least-square minimization:

$$F(\mathbf{p}) = \sum_{\substack{i,j,k \\ i \neq j \neq k \neq i}} \left[\phi_k^{ij}(\mathbf{p}) - U_k^{ij}\right]^2 \to \min, \tag{17}$$

where U_k^{ij} and $\phi_k^{ij}(\mathbf{p})$ are the measured and computed potentials at the kth electrode for the i and j injection electrodes. $\phi^{ij}(\mathbf{p})$ is a solution of the forward problem corresponding to parameter $\mathbf{p}$ for the location of the internal boundaries.

For minimizing (17) we used Powell's method [2] and a genetic algorithm [3]. In the genetic algorithm the vector of parameters was converted to a bit string by a standard procedure [4].

7 Numerical Results

To check the accuracy of the singular BEM we performed several tests for domains bound by a cube or a sphere with various numbers of panels and nodes. We then obtained analytical solutions using a given distribution of sources and sinks in space and compared them with those computed using the singular BEM.

The computational surface mesh for a cube was generated with 590 nodes and 1176 panels. Figure 1 shows the comparison node by node of the numerical solution

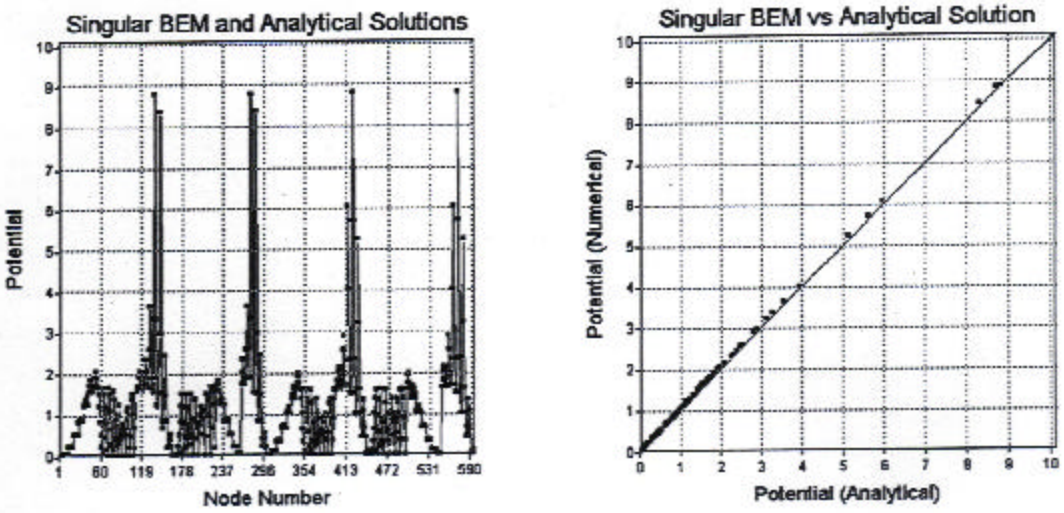

Figure 1: The absolute value of the electric potential on the cube surface created by two point electrodes. Results obtained using the singular BEM (squares) and the known analytical solution (solid line).

versus the analytical solution. Note that the relative r.m.s. error for this case is 2.4%. The solution of the same problem using the standard BEM shows an error of about 10% , due to violation of condition (13) (the norm of the non-orthogonal component of Y is about 10-15% of the norm of Y depending on the locations of the sinks and sources).

The number of calls of the forward problem solver depends on the dimension of the vector $\mathbf{p}$ and on the selected minimization strategy. Usually calculus-based minimization algorithms, such as Powell's method, show a high initial convergence rate (see Figure 2). However, they may not converge to the global minimum, especially for large dimensions of $\mathbf{p}$. This is the case for example for the reconstruction of two spheres. In contrast, the genetic algorithm showed in all our numerical experiments a lower convergence rate, but a very good convergence to the exact solution (Figure 2). Examples of reconstruction of two spheres and an ellipsoid embedded in a cube are shown in Figure 3.

8 Conclusions

The singular BEM has shown a good accuracy when compared with analytical solutions for cubic and spherical domains. The comparisons showed substantial improvement when compared with the standard BEM. The singular BEM was incorporated into the EIT algorithm and reconstructions of 3D zero conductivity regions were carried out. The speed up of the computations enabled use with optimization strategies such as genetic algorithms which require tens of thousands of calls of the forward problem solver.

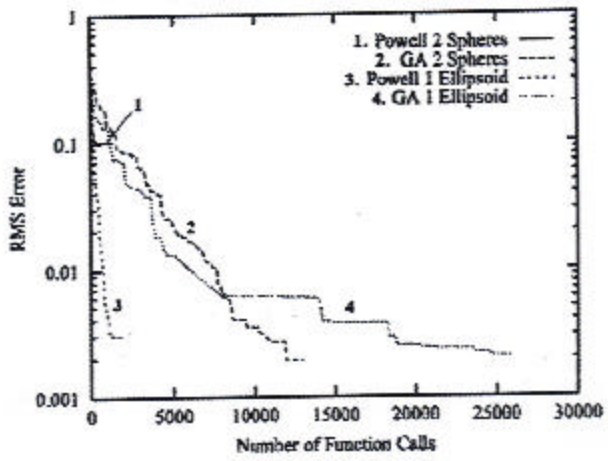

Figure 2: The convergence histories for the Powell and genetic algorithm with the singular BEM forward problem solver for two spheres and an ellipsoid.

9 Acknowledgment

This study has been supported by the National Science Foundation Phase II SBIR grant DMI 9806707.

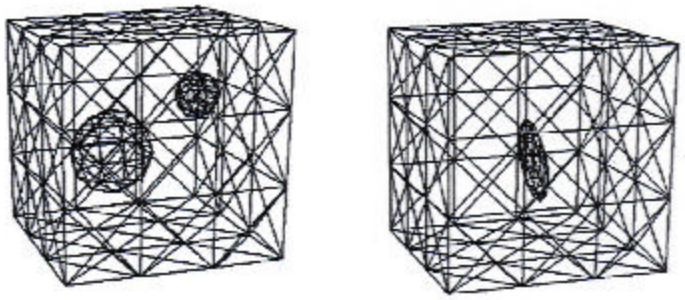

Figure 3: Exact and converged solution using reconstructions based on the singular BEM and a single-objective genetic algorithm for 2 spheres and an ellipsoid. The reconstructed solutions are practically on top of the correct solutions.

References

[1] Duraiswami, R., Chahine, G.L., and Sarkar, K. (1997) "Boundary element techniques for efficient 2-D and 3-D electrical impedance tomography." Chem. Eng. Sci., 52(13), 2185-2196.

[2] Press, W.H., Teukolsky, S.A., Vetterling, W.T., and Flannery, B.P. (1992) "Numerical Recipes." Cambridge University Press, 2nd ed.

[3] Goldberg D.E. (1989) "Genetic Algorithms in Search, Optimization & Machine Learning." Addison Wesley.

[4] Chahine, G.L., Gumerov, N.A., Chao, C.-T., and Goumilevski, A.G. (1998) "Efficient Electrical Impedance Tomography Using Boundary Element Methods." DYNAFLOW, INC. Phase II NSF SBIR Technical Report 96008-1.

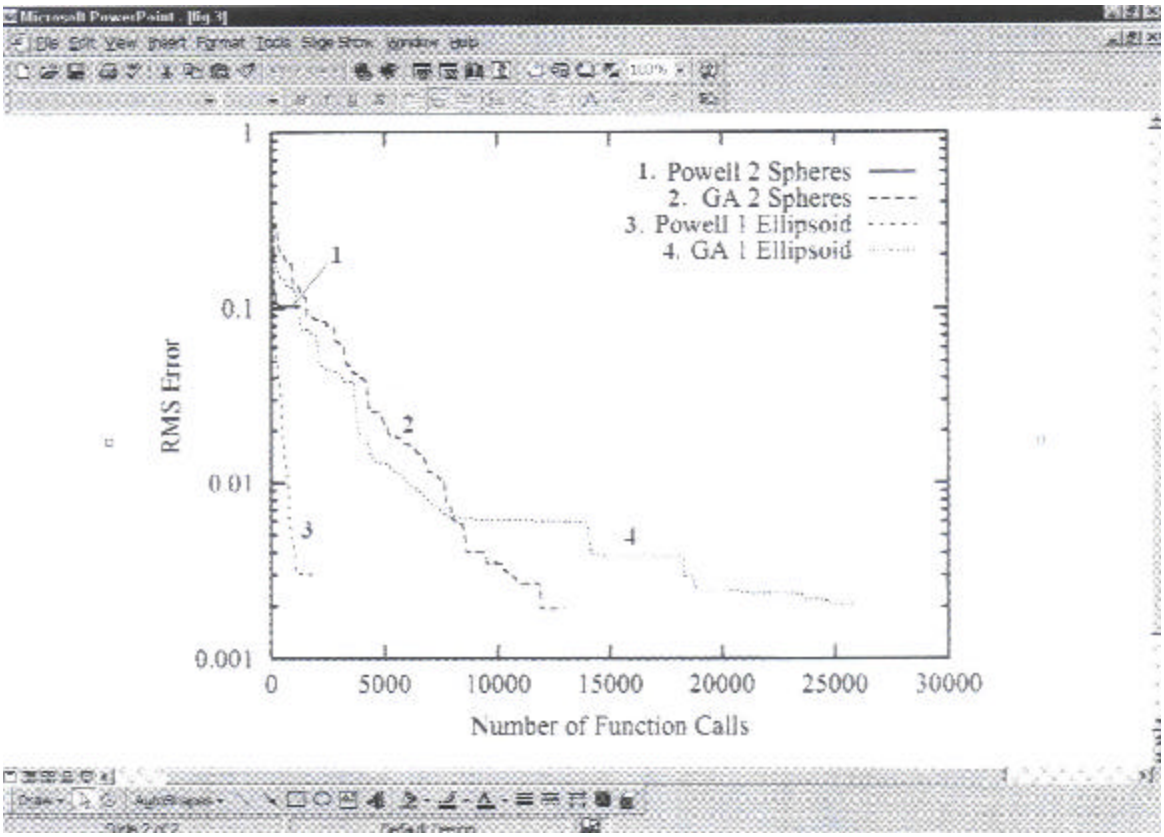
1. Powell 2 Spheres
2. GA 2 Spheres
3. Powell 1 Ellipsoid
4. GA 1 Ellipsoid
RMS Error
1
0.1
0.01
0.001
0
5000
10000
15000
20000
25000
30000
Number of Function Calls

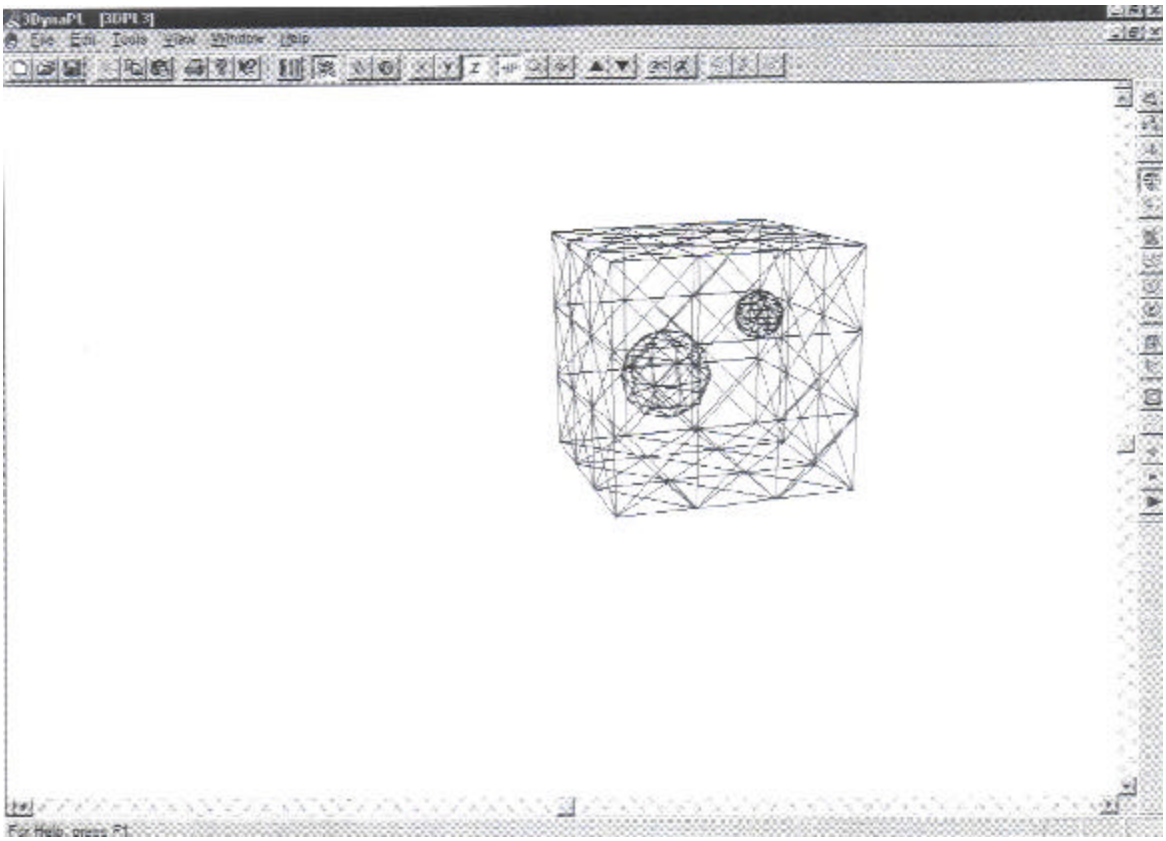
3DynaPL [3DPL3]
File Edit Tools View Window Help
For Help, press F1

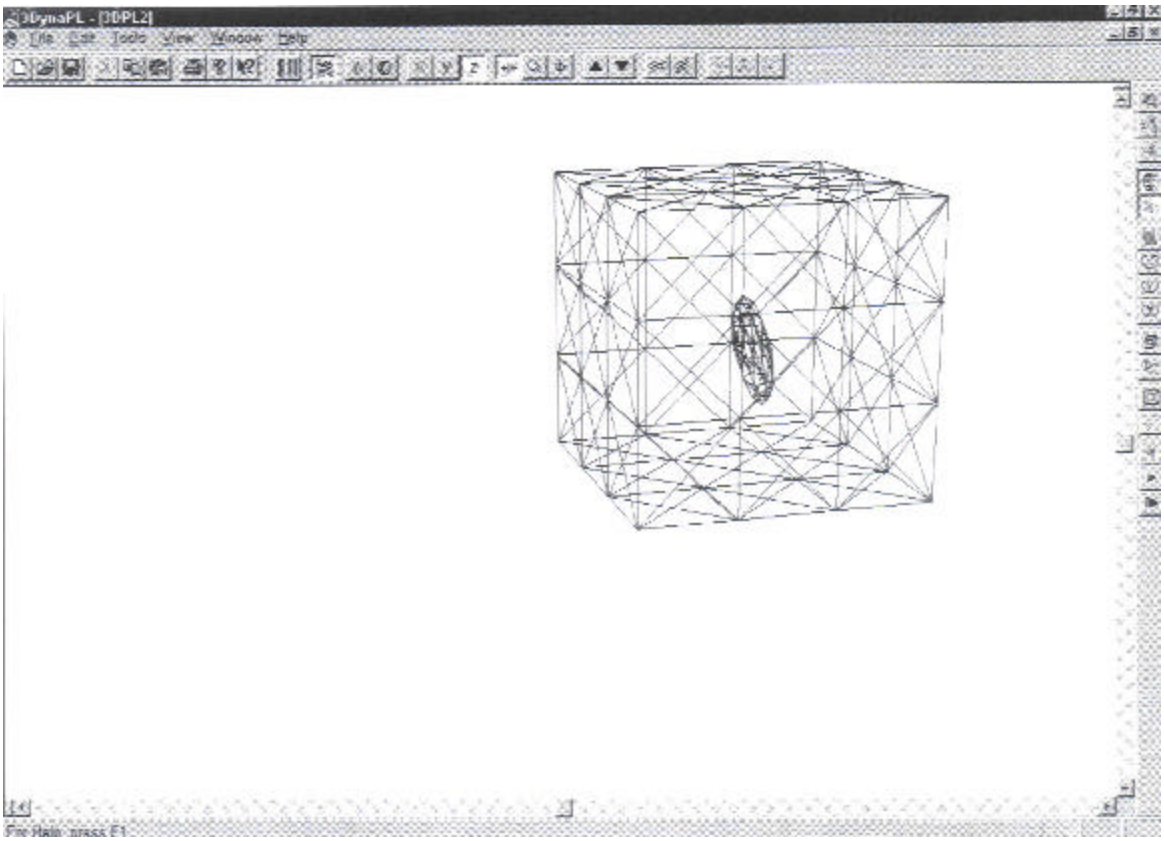
3DynaPL - [3DPL2]
File Edit Tools View Window Help
For Help, press F1